Theory of electron transport through a periodic array of devices with transverse exit leads

John L. Bohn*
JILA and Quantum Physics Division, National Institute of Standards and Technology, Boulder, Colorado 80309
(Received 28 October 1996; revised manuscript received 21 February 1997)

We introduce a periodic array of nanoscale semiconductor devices, where *each device* contains a transverse lead into which conduction electrons can be deflected. These ''deflective'' arrays exhibit a unique resonance structure with respect to electrons traveling the length of the array: coefficients for reflection and transmission through the array can peak *simultaneously* at resonance, unlike the analogous case in superlattices. We focus in particular on an array of T-shaped devices, similar to those grown recently by epitaxial methods, and characterized by perfection of structure and extremely small size. The T-array's nonlinear *I-V* characteristics, along with its multiple paths for electron flow, may lead to interesting switching applications. [S0163-1829(97)00232-4]

I. INTRODUCTION

Semiconductor nanoscale devices afford an endless variety of scattering geometries for ballistically propagating conduction electrons. Typical geometries of interest for device applications consist of narrow quantum wires that serve as leads into and out of a scattering region whose shape is engineered to yield a desired conductance through the device. Such scattering regions include arrays of T-shaped ''stubs''[1] or more elaborate rectangular geometries;[2] curvilinear shapes, such as stadiums, that incorporate ''quantum chaos'';[3] bent quantum wires that localize electron density in their bends;[4] and pairs of parallel quantum wires connected by a transverse quantum wire.[5]

Viewed as a scattering problem, the shape of an individual device influences the transmission coefficient from the device's input lead to its output lead, yielding typically a set of resonances where the transmission abruptly drops at certain scattering energies. An array of equally spaced identical devices yields instead a ''miniband'' structure, which influences conductance properties by creating band gaps, ranges of incident electron energy within which the transmission probability nearly vanishes. These band gaps are governed primarily by the spacing between devices, since the propagating electrons see essentially a periodically modulated potential, much like the Kronig-Penney model of one-dimensional band structure.[6] Device arrays considered so far comprise a single input lead feeding a single output lead, meaning that the entire incident electron flux appears as scattered flux in either the input lead or the output lead. (Here we consider only ballistic transport and ignore dissipation into phonon modes of the device.) The theoretical treatment of these devices concerns then the determination of reflection and transmission probabilities, handled easily by transfer matrices or analogous methods (e.g., Ref. 1).

This paper approaches instead a periodic array, in which *each* device in the array incorporates a transverse lead through which electron flux can exit. Figure 1 sketches the prototype device considered in this paper. Each element of the array, as pictured in Fig. 1(a), consists of a T-shaped quantum wire, of widths a and b in its vertical and horizontal arms, respectively. Unlike the stubs considered in Ref. 1, here the vertical arm of the T is assumed long enough that any electron flux entering this arm is effectively lost. The centers of the T's are spaced by a distance d, as in Fig. 1(b), forming a periodic array with a finite number of members, N_T. The transverse leads afford the possibility of *deflecting* current out of the array altogether; we therefore refer to such an array as deflective. The deflective nature of an array strongly influences its miniband structure, as exemplified by scattering resonances where reflection and transmission coefficients through the array can simultaneously peak. These resonances, and some of their observable consequences, form the core of this paper.

An array of T's like that pictured in Fig. 1 might be etched using standard lithography techniques. There is, however, a more suitable procedure for accurately forming the array, namely, the cleaved-edge-overgrowth (CEO) process.[7] In this process the vertical arms are first grown as alternating GaAs-$Al_xGa_{1-x}As$ layers by molecular beam epitaxy. The resulting crystal is then cleaved along a plane orthogonal to the vertical arms, and a new layer of GaAs grown to form the

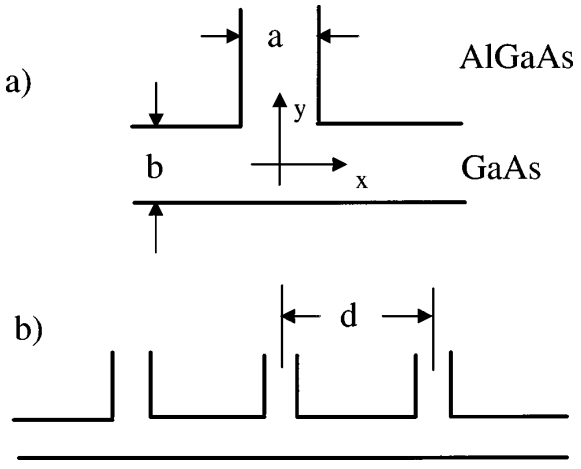

FIG. 1. The device. (a) shows a T-shaped structure formed of GaAs embedded in $Al_xGa_{1-x}As$. Electrons propagate ballistically within the T-shaped region. (b) shows an array of such devices, placed at equal intervals d. The array as a whole is termed ''deflective,'' because of the possibility of deflecting conduction electrons into each T's vertical lead.

horizontal arms. (The resulting array of T's then has translational symmetry in the direction orthogonal to the plane of Fig. 1; we disregard in this paper motion out of this plane.) Epitaxial techniques imply both a high degree of perfection in the structure and an extremely small size, with a and b typically of order 10 nm. For these reasons, CEO-grown T's have been considered as high-quality quantum wires localized at the crux of each T (Ref. 8) and as exciton lasers.[9] In addition, by reversing the roles of GaAs and $Al_xGa_{1-x}As$ in Fig. 1, transport through precisely defined two-dimensional (2D) superlattices has been studied. In this case the electrons tunnel across the T's and are classically allowed only in the space between T's.[10] The present work appears to be the first to consider transport through the directly connected T's themselves.

The multiplicity of exit leads in the array in Fig. 1 implies that a theoretical treatment in terms of transfer matrices proves inadequate. Rather, a full scattering matrix for each T must be constructed; these can then be strung together in a convenient way to describe the scattering properties of the entire array. We calculate scattering matrices using an ''R-matrix'' formalism that has been enormously successful in atomic scattering calculations, and which is sufficiently general to handle much more elaborate systems than the T's considered here. In addition, the method reported here for connecting the scattering matrices of individual T's should find wide application in similar problems.

II. MODEL AND METHOD

The model in this paper assumes that the array pictured in Fig. 1 is crafted from a GaAs-$Al_xGa_{1-x}As$ heterostructure, as has been the case in structures previously grown by CEO. Accordingly, it assumes an effective electron mass of $m^*=0.067m_e$, where m_e stands for the bare electron mass. The model also assumes that the electron is contained within the T by infinitely high potential barriers, and that individual electrons propagate ballistically through the entire array. These assumptions pose no serious restrictions, since the present aim is to assess the impact of the open vertical arms on electron transport.

A description of the scattering of a single electron through the array in Fig. 1 requires solutions to the Schrödinger equation

$$-\frac{\hbar^2}{2m^*}\vec{\nabla}^2\psi=E\psi \tag{2.1}$$

for the range of scattering energies E of interest, subject to vanishing boundary conditions on the perimeter of the array. In each lead the wave function is separable and can be expressed as linear combinations of functions $h_i(\xi)f_i^{\pm}(E;\eta)$, where ξ represents the coordinate transverse to a given lead, and η the coordinate along the lead, increasing in the direction away from the array. The (normalized) transverse wave function in mode n_i reads

$$h_i(\xi)=\sqrt{\frac{2}{w}}\cos\left(\frac{n_i\pi}{w}\xi\right) \tag{2.2}$$

for a lead of width w ($=a$ or b). The longitudinal wave function takes the form

$$f_i^{\pm}(E;\eta)=\frac{1}{\sqrt{2k_i}}\exp(\pm ik_i\eta) \tag{2.3}$$

whose wave number k_i satisfies

$$\frac{\hbar^2}{2m^*}\left[\left(\frac{n_i\pi}{w}\right)^2+k_i^2\right]=E. \tag{2.4}$$

If $k_i^2>0$, then f_i^- and f_i^+ stand for incoming and outgoing traveling waves, respectively, and channel i is energetically ''open.'' Otherwise, the channel is ''closed,'' and the functions $f_i^{\mp}$ become the exponentially growing and decaying functions $\exp(\pm\kappa\eta)$ by the substitution $k\rightarrow i\kappa$, with $\kappa>0$.

Scattering of an electron by the array is described at each incident energy E by a scattering matrix S, whose element S_{ji} represents the (complex) amplitude for the electron to exit the array in channel j, given a unit incident flux in channel i. These scattering wave functions far from the array therefore take the form[11]

$$h_j(\xi)[f_j^-(E,\eta)\delta_{ji}-f_j^+(E,\eta)S_{ji}(E)]. \tag{2.5}$$

The following subsections construct the scattering matrix for the array in two steps, by first computing the scattering matrix for a single T, then by stringing these matrices together to obtain the full scattering matrix.

A. Scattering matrix for a single T

We determine a single-T's scattering matrix by the R-matrix method invented by Wigner in the context of nuclear scattering theory,[12] and extensively developed for use in atomic scattering theory (See, for instance, the reviews in Refs. 13–15) The mathematical underpinning of this method is sketched in Appendix A. Briefly, the method solves the Schrödinger equation separately in two regions: an ''outer'' region where the wave function consists of superpositions (2.5) of scattering wave functions; and an ''inner'' region, the T itself, where where the wave function is more complicated and must be determined numerically. Matching these solutions and their derivatives across the boundary between inner and outer regions identifies the scattering matrix in Eq. (2.5).

We first identify the inner region of the T as the rectangular ''box'' $|x|\leq a/2$, $|y|\leq b/2$ where all the leads overlap (this is the region denoted ''A'' in Appendix A). Within this box we seek, for each value of E, solutions ψ_β vanishing along the line $y=-b/2$ and having a constant outward normal logarithmic derivative $-b_\beta=\psi_\beta^{-1}(\partial\psi_\beta/\partial n)$ along the other three sides. Here $\partial/\partial n$ stands for the outward normal directional derivative through the box's boundary. These logarithmic derivatives then provide a convenient set of boundary conditions for matching the leads' wave functions (2.5), requiring a matching only in the longitudinal coordinate η. (This two-step approach has proven very useful in more elaborate settings, such as electron-atom or electron ion scattering processes, where the atom or ion is treated within a closed three-dimensional inner region. Typically, the logarithmic derivatives vary much more slowly with energy than do the resulting scattering matrices, which exhibit narrow resonances; computational effort is thereby reduced.)

The constant-logarithmic-derivative solutions can generally be computed usefully with finite element techniques.[16] In the simple geometry of the present example we use instead a basis set expansion, as derived in Appendix A. The basis consists primarily of functions $\phi_k^{(v)}$ that vanish on the box boundaries,

$$\phi_k^{(v)} = \sqrt{\frac{2}{a}}\cos\left(\frac{n\pi}{a}x\right)\sqrt{\frac{2}{b}}\cos\left(\frac{m\pi}{b}y\right). \tag{2.6}$$

These functions form a complete set within the inner region, and can thus account for the full two-dimensional shape of the scattering wave function. To be useful computationally, however, they must be complemented by basis functions $\phi_k^{(nv)}$ nonvanishing on the box's surface. For example,

$$\phi_k^{(nv)} = \sqrt{\frac{2}{a}}\cos\left(\frac{n\pi}{a}x\right)\sqrt{\frac{2}{b}}\sin\left[\frac{\pi}{2b}\left(y+\frac{b}{2}\right)\right] \tag{2.7}$$

is nonzero along the upper egde of the box $y=b/2$; and similarly for the other two edges. These additional basis functions allow for finite values of the logarithmic derivatives b_β on the box's surface. Similar overcomplete bases are standard in applications of the R-matrix method to atomic scattering problems,[15] but cause no harm, since there is no requirement that the basis set be orthogonal.

Denoting basis functions generically by ϕ_k, we expand the solutions as $\psi_\beta = \Sigma_k \phi_k Z_k^\beta$. Using this expansion as a trial wave function in a variational expression for the logarithmic derivative (Appendix A) yields a generalized eigenvalue problem for the eigenvalues b_β and eigenvectors Z^β:[17]

$$\Gamma \vec{Z} = b\Lambda \vec{Z}, \tag{2.8}$$

where

$$\Gamma_{kk'} = \frac{2m^*}{\hbar^2}\int_A \phi_k(E-H)\phi_{k'}dA - \int_l \phi_k \frac{\partial \phi_{k'}}{\partial n}dl \tag{2.9}$$

involves an integral over the area A of the box as well as a line integral over its perimeter l, and H stands for the electron's Hamiltonian inside the box. The right-hand matrix is given by the line integral

$$\Lambda_{kk'} = \int_l \phi_k \phi_{k'} dl. \tag{2.10}$$

These matrices are easily evaluated in the potential-free region inside the box. Typically 10–20 basis functions already suffice for convergence of the eigenvectors ψ_β.

The number of independent solutions to the generalized eigenvalue problem (2.8) equals the rank of the matrix Λ,[18] which in turn equals the number of basis functions nonvanishing on the box's boundary. This number should in general coincide with the total number N of channels i in the leads. On the surface of the box, each solution ψ_β, along with its normal derivative, can be expressed as a linear combination of scattering solutions (2.5),

$$\psi_\beta = \sum_{ij} h_j[f_j^- \delta_{ji} - f_j^+ S_{ji}]N_i^\beta,$$

$$\frac{\partial \psi_\beta}{\partial n} = -b_\beta \psi_\beta = \sum_{ij} h_j\left[\frac{\partial f_j^-}{\partial n}\delta_{ji} - \frac{\partial f_j^+}{\partial n}S_{ji}\right]N_i^\beta. \tag{2.11}$$

Here the coefficients N_i^β serve to connect the normalizations of wave functions inside and outside the box. Projection onto each of the N nonvanishing basis functions $\phi_k^{(\mathrm{nv})}$ in turn yields a system of $2N^2$ equations for the $2N^2$ matrix elements S_{ji} and N_i^β:

$$Z_k^\beta = \sum_{ij}\left(\int_l \phi_k^{(\mathrm{nv})} h_j dl\right)[f_j^- \delta_{ji} - f_j^+ S_{ji}]N_i^\beta,$$

$$-b_\beta Z_k^\beta = \sum_{ij}\left(\int_l \phi_k^{(\mathrm{nv})} h_j dl\right)\left[\frac{\partial f_j^-}{\partial n}\delta_{ji} - \frac{\partial f_j^+}{\partial n}S_{ji}\right]N_i^\beta. \tag{2.12}$$

In practice, each nonvanishing basis function $\phi_k^{(\mathrm{nv})}$ projects onto *only one* scattering wave function h_i, since in the transverse direction both sets consist of orthogonal cosines. This circumstance further simplifies the solutions of Eq. (2.12) in the present case.

B. Connection of multiple T's

Once the scattering matrix for a single T is determined by the method of the previous section, the scattering matrices for a string of T's may then be fused to yield the scattering matrix for the entire array. For simplicity we will illustrate this connection for a pair of T's, but the method is of course completely general.

First let us denote the leads in each T by the letters L,R, U, to distinguish the left, right, and upper leads for a T in the orientation shown in Fig. 1(a). One T, identified by the number 1, is centered at the origin of the coordinate system shown, while the second, identified by the number 2, is centered at $x=d$. The *most general* form of the wave function in any of the six leads is a superposition of incoming and outgoing waves. Let L_1^+, for instance, stand generically for the set of coefficients of the f^+ wave functions in lead L of T number 1, and similarly for the rest of the leads. The incoming (ψ^+) and outgoing (ψ^-) wave functions for each T are then characterized by column vectors divided into three blocks:

$$\psi_{1,2}^\pm = \begin{pmatrix} L_{1,2}^\pm \\ R_{1,2}^\pm \\ U_{1,2}^\pm \end{pmatrix}. \tag{2.13}$$

In terms of the single-T scattering matrix S, the full scattering matrix for all six leads relates incoming and outgoing waves by

$$\begin{pmatrix} \psi_1^+ \\ \psi_2^+ \end{pmatrix} = \begin{pmatrix} S & 0 \\ 0 & S \end{pmatrix}\begin{pmatrix} \psi_1^- \\ \psi_2^- \end{pmatrix}, \tag{2.14}$$

which exhibits a block-diagonal structure, indicating that the T's remain independent to this point in the derivation.

Once the two T's are placed side by side, the leads R_1 and L_2 become unobservable, that is, they no longer extend to large distances from the T's. This circumstance cuts the number of physical leads down to four. The effect of wave propagation in channels within the unobservable (''*u*'') leads on scattering among channels in the observable (''*o*'') leads can be assessed by a formalism originally due to Feshbach.[19] In Ref. 19, the unobserved channels consisted of bound states of a scattering complex, which give rise to resonant states when coupled to a scattering continuum. Similarly, arrays of T's will exhibit resonant states based on quasi-bound states of the array, i.e., whenever the electron's wavelength along the wires becomes comparable to an integral multiple of d.

To implement this formalism, it is convenient to rearrange the vectors (2.13) according to observable channels $\{L_1,U_1,U_2,R_2\}$ and unobservable channels $\{R_1,L_2\}$, in particular defining

$$\psi_u^+=\begin{pmatrix} R_1^+ \\ L_2^+ \end{pmatrix}, \quad \psi_u^-=\begin{pmatrix} L_2^- \\ R_1^- \end{pmatrix}. \tag{2.15}$$

The scattering relation in Eq. (2.14) then takes the form

$$\begin{pmatrix} \psi_o^+ \\ \psi_u^+ \end{pmatrix}=\begin{pmatrix} S_{oo} & S_{ou} \\ S_{uo} & S_{uu} \end{pmatrix}\begin{pmatrix} \psi_o^- \\ \psi_u^- \end{pmatrix}. \tag{2.16}$$

(The detailed arrangement of the observable components $\psi_o^{\pm}$ is irrelevant for the present purposes.) The unobserved leads are thus coupled (so far only to themselves) by the S_{uu} portion of the scattering matrix. These leads satisfy an additional relation arising from the fact that any flux emerging from R_1 must appear in L_2, and vice versa. This condition is met by matching, in each transverse mode h_i, the wave functions

$$R_1^-\exp[-ikx]-R_1^+\exp[ikx],$$

$$L_2^-\exp[ik(x-d)]-L_2^+\exp[-ik(x-d)], \tag{2.17}$$

and their x derivatives, at $x=d/2$.

This matching implies a further constraint on the amplitudes in the unobservable leads:

$$\psi_u^+=-\exp(-ikd)\psi_u^-, \tag{2.18}$$

embodying the phase gained by an electron traveling the distance d between T's. Note that for energetically closed channels the exponential becomes instead $\exp(\kappa d)$, which accounts for an evanescent wave between T's. Writing out Eq. (2.16) in components and employing the matching condition (2.18) allows the construction of a ''reduced'' scattering matrix that connects only the channels in the observable leads:

$$\psi_o^+=S^{\rm red}\psi_o^-, \quad S^{\rm red}=S_{oo}-S_{ou}[\exp(-ikd)+S_{uu}]^{-1}S_{uo}. \tag{2.19}$$

The inverse in this equation implies a resonance when the matrix $\exp(-ikd)+S_{uu}$ becomes nearly singular.

For a larger assembly of T's the reduced scattering matrix is formed in the same way. First, the amplitudes in all unobservable leads are collected, then those in adjacent T's are related through matching conditions analogous to Eq. (2.17).

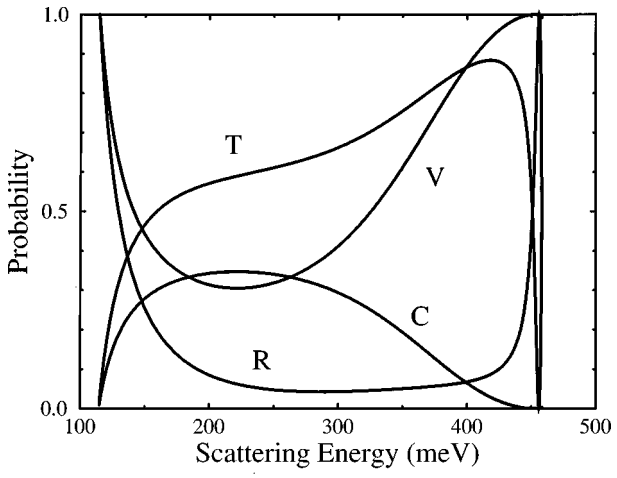

FIG. 2. Scattering probabilities between the various leads of a single T, with $a=b=7$ nm, versus scattering energy. The letter codes stand for *T*, horizontal straight-through transmission; *R*, horizontal reflection; *V*, vertical reflection; and *C*, probability to scatter electrons ''around the corner.''

Note that each T is connected only to its nearest neighbors on either side, so the scattering matrices involved have a sparse structure. This circumstance greatly eases the computational load, especially of the matrix inversion in Eq. (2.19).

One final detail: the reduced scattering matrix $S^{\rm red}$ incorporates all channels in the observable leads, including the energetically closed channels that contain exponential divergences away from the array. However, the choice $f_i^-=\exp(\kappa_i\eta)$ in closed channels i implies that only the scattering wave functions (2.5), with i representing a closed channel, contain such divergences. Put another way, the only elements S_{ij} of the scattering matrix relevant to physical scattering are those in which i and j both refer to open channels.

III. SCATTERING PROPERTIES

In this section we present some fairly typical results on single-T structures and especially on small arrays of T's, drawing attention to their unique scattering features. For concreteness, we consider T's whose horizontal and vertical leads are both 7 nm wide, and which are spaced 22 nm apart. We emphasize that these are realistic dimensions for the CEO-grown T structures reported in Ref. 7. Most of the results can be understood in terms of the electron's longitudinal DeBroglie wavelength in mode n of the incident channel,

$$\lambda=\frac{2\pi}{\sqrt{\frac{2m^*}{\hbar^2}E-\left(\frac{n\pi}{b}\right)^2}}. \tag{3.1}$$

Scattering features tend to occur at energies where a multiple of $\lambda/2$ coincides with one of the dimensions a,b, or d.

A. Scattering in a single T

Figure 2 presents the various scattering probabilities for an electron passing through a single T, in the energy range between $E_1=\hbar^2\pi^2/2m^*a^2=114.54$ meV and E_2

$=4\hbar^2\pi^2/2m^*a^2=458.16$ meV. These energies are the thresholds for propagation of the first and second modes along the leads; each lead thus possesses only a single open channel within the energies presented in Fig. 2. In this figure, ''T'' and ''R'' stand for transmission and reflection straight through in the horizontal direction; ''V'' stands for the probability for an electron incident in the vertical lead to be reflected back into the vertical lead; and ''C'' stands for the probability of ''turning the corner,'' i.e., of entering in a horizontal lead and exiting through the vertical (or vice versa).

At energies just above the threshold E_1, electrons incident in either horizontal or vertical leads are reflected with nearly unit probability. In this limit the incident electron's longitudinal wavelength λ greatly exceeds the size of the T, so that the T's only impact on the electron is a sudden boost in kinetic energy when the electron is no longer confined within the lead. The threshold propagation may then be regarded as one-dimensional free propagation with a sudden potential drop at the region of the T. Elementary methods[20] demonstrate that the reflection coefficient for this process becomes unity at threshold.

At energies above this threshold region, the reflection probability for the horizontal arms drops dramatically, as propagation straight through the T becomes increasingly likely. Moreover, the coupling between horizontal and vertical leads increases, exhibiting a maximum near $E\sim 220$ meV, at which energy $\lambda/2$ nearly matches the width of the vertical channel. This circumstance is optimal for sending electron flux around the corner, but the quasi-resonance thus generated appears very broad; flux leaks fairly easily from horizontal into vertical leads. Notice also that the reflection coefficient for scattering from the vertical lead into itself remains fairly high throughout, since the incoming wave really has a solid wall from which to reflect.

The probability for scattering from a horizontal lead into the vertical lead tends to vanish at energies approaching the threshold E_2. At these energies, $\lambda/2$ becomes too short to match conveniently the lowest mode in the vertical lead, but λ gets close to matching the second mode. In fact, at an energy of $E\sim 455$ meV, just 3 meV below threshold, this second mode is resonantly excited, sending the horizontal lead's reflection coefficient abruptly to unity. The vertical lead's reflection coefficient also notes the resonance, but as a phase shift only, which does not appear in the probability plotted in Fig. 2.

B. Periodic array of T's

Our main interest in arrays of T's lies in the propagation of electrons through the entire array, horizontally from left to right. The presence of the uncapped vertical leads, i.e., the array's deflective nature, deeply affects its scattering properties. Figure 3 shows the reflection (R) and transmission (T) probabilities through an array consisting of eight T's spaced at 22 nm intervals, for the same energy range as Fig. 2. The reflection probability is dominated by a series of peaks superimposed on the single-T reflection probability. These peaks lie at energies where the wavelength λ satisfies the condition $n\lambda/2=d$ for some integer n. Consequently, the scattering wave function possesses nodes at the intersection

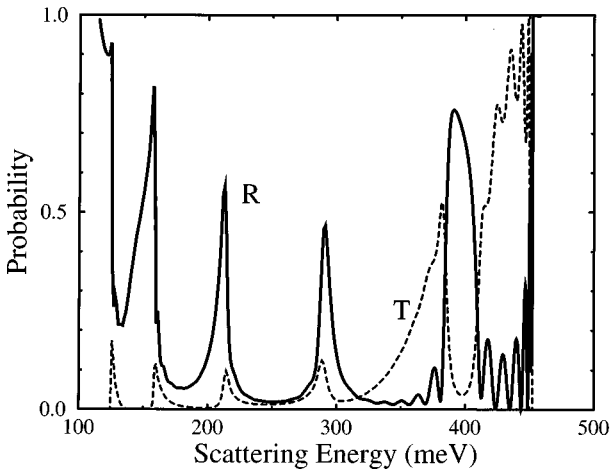

FIG. 3. Reflection (R, solid line) and transmission (T, dashed line) probabilities for an electron incident from one end of an array of eight T's, spaced $d=22$ nm apart. For scattering energies $E<350$ meV, R and T peak simultaneously at resonance energies governed by the spacing d. For $E>350$ meV, R and T resemble more closely the probabilities for a one-dimensional array.

of the horizontal arm with each vertical lead, greatly reducing the flux lost to vertical leads. The array then acts like a one-dimensional array, which exhibits enhanced Bragg reflection at these wavelengths.

Between each pair of these main peaks lie N_T-2 additional peaks, generated by wave functions whose wavelength λ fits an integral number of times into the whole array of length $(d-1)N_T$, but which may not vanish at every vertical lead. Reflection at the corresponding energies is therefore generally weaker than at the main peaks, although the peaks are stronger at low and high energies, where the individual T reflection coefficients are the largest. At intermediate energies these additional peaks are not visible on the scale of Fig. 3.

Due to the deflective nature of the array, the reflection and transmission probabilities do not satisfy $R+T=1$. On the contrary, there are large ranges of energy where both R and T remain small, and most of the incident flux spills out the vertical leads. For $E<350$ meV the only way an electron can travel through the entire array is if the flux deflected into the vertical leads is shut off, which happens at the resonant energies. The T array has thus the property that its reflection and transmission probabilities *peak simultaneously* at certain resonances, which could not happen in a superlattice or other nondeflective array.

At energies above ~ 350 meV, a different phenomenon occurs. Here the vertical lead in each T ''decouples itself,'' as the probability within each T to scatter around the corner drops to zero. In this case the horizontal propagation begins to mimic an ordinary one-dimensional array. In particular, the condition $R+T=1$ is more nearly satisfied. As is typical for a one-dimensional array, the transmission probability is nonnegligible, except at the resonance condition $n\lambda/2=d$, which occurs at energy $E=404$ meV for $d=22$ nm. This energy identifies a forbidden band, wider than the scattering resonances at lower energies. (Notice that there is another narrow band near the E_2 threshold, associated with the $E=455$ meV scattering resonance discussed above.) The ar-

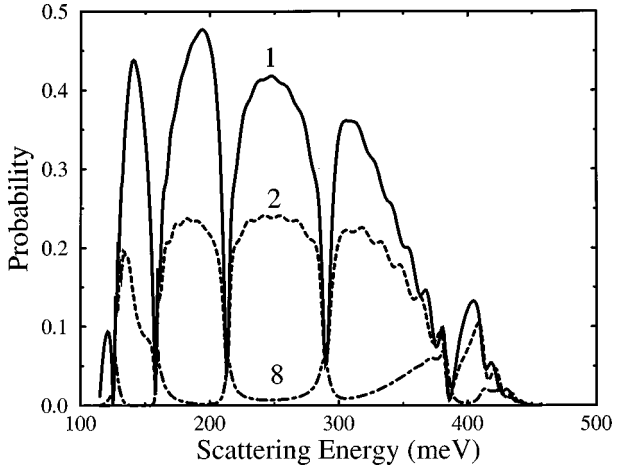

FIG. 4. Probabilities for an electron incident on one end of an array of eight T's to scatter into the first (1), second (2), or eighth (8) vertical lead it encounters, under the same conditions as in Fig. 3.

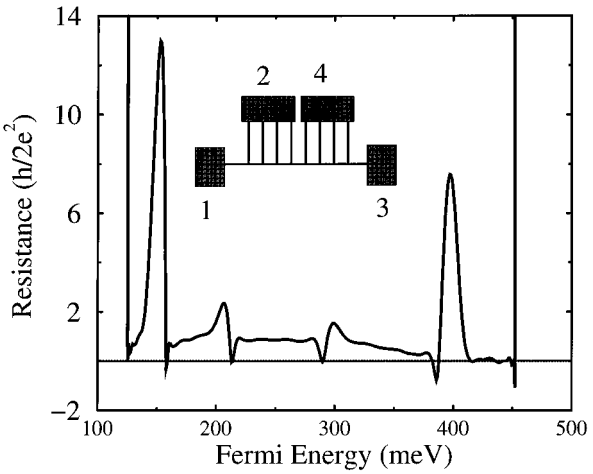

FIG. 5. Inset: schematic of an eight-T array, with four metallic terminals (shaded boxes) attached. The main figure plots the zero-temperature resistance of the array, versus the Fermi energy E_F of the terminals. This resistance represents the ratio of the voltage across terminals 2 and 4, to the current passing between terminals 1 and 3. When E_F nears a resonance, the measured resistance can become negative.

ray thus exhibits a transition from quasi-two-dimensional behavior below 350 meV, to quasi-one-dimensional behavior above 350 meV.

As the number of T's increases the contrast between the low- and high-energy behavior of R and T continues. First, the reflection resonances below 350 meV persist, becoming somewhat narrower and higher. Beyond $N_T \sim 20$ they change very little, indicating that full reflection takes place within the first 20 T's or so. The corresponding transmission resonances dwindle to insignificance at this point, owing to the increasing difficulty of propagating through the entire array. Above 350 meV, the band structure persists, with the transmission probability diminishing only slowly as more T's are added. The forbidden band becomes more sharply defined, with T vanishing completely for 390 meV $< E <$ 410 meV.

Finally, Fig. 4 shows, for the same eight-T array, the probabilities for scattering into the first, second, and eighth vertical lead. Approximately twice as much of the lost flux leaves through the first vertical lead as through the second; generally the leads farther from the incident lead leak less flux, because they receive less in the first place. The effect of resonances tends to reverse this general trend. Transmission to the first vertical lead diminishes at the scattering resonances, thereby plugging the biggest leak. Transmission to the last lead actually increases, however, for the same reason that transmission out the right-hand lead increases: only on resonance does the electron navigate the entire length of the array. Moreover, transmission through the first and last leads become approximately equal on resonance, indicating that all vertical leads are approximately equivalent when decoupled from horizontal motion.

IV. ELECTRICAL RESISTANCE

The scattering properties described above influence the flow of electrons through a deflective array of T's, thereby influencing the effective resistance of the array, considered as a circuit element. In one dimension, electrical conductance has long been known to follow from the transmission and reflection properties of random scattering events in a long straight wire[21] or of scattering by a device embedded in the wire.[22] These results have been further generalized to devices with multiple input and output leads, as is relevant here.[23]

We consider a particular wiring arrangement, depicted in the inset to Fig. 5. Here four terminals are connected to the various leads in the array: terminals 1 and 3 connect to the left- and right-hand leads, while terminals 2 and 4 each connect to half the vertical leads on the left- and right-hand sides of the array. We assume all terminals are composed of the same material, with a common Fermi energy E_F. Each terminal i serves as a reservoir of electrons, filled to its chemical potential μ_i, as governed in equilibrium by the currents and voltages at the terminals. Generally speaking, μ_i remains close to E_F so that electrons enter the device with energy $E \sim E_F$.

Reference 23 relates the current flowing into the device through lead i to the chemical potentials in all other leads by the probabilities R_{ii} and T_{ij} for scattering a unit current from lead i back into lead i or into lead j, respectively:

$$I_{\text{lead}i} = \frac{2e}{h}\left[(1-R_{ii})\mu_i - \sum_{i \neq j} T_{ij}\mu_j\right]. \tag{4.1}$$

Here e stands for the electron's charge, and h for Planck's constant. The quantities R_{ii} and T_{ij} are the squares of the relevant scattering matrix elements evaluated at energy E_F. For the present purposes, the relevant quantities are the *total* currents flowing into each terminal, involving the sum of the currents in the relevant leads. In terminals 2 and 4 this implies currents

$$I_2 = \sum_{i \in \text{terminal } 2} I_{\text{lead}i}, \quad I_4 = \sum_{i \in \text{terminal } 4} I_{\text{lead}i}. \tag{4.2}$$

Likewise, the terminals are equipotentials, meaning that the chemical potential is the same in any lead connected to a given terminal. These circumstances allow the definition of

effective scattering probabilities R_{ii} and T_{ij} for the physically relevant currents I_i and chemical potentials μ_i in the four terminals i. These quantities are then related by equations of the same form as Eq. (4.1), which must be solved subject to boundary conditions describing the potential differences and currents in a given experimental setup.

A typical four-terminal experiment consists of external circuits connected between terminals 1 and 3, and between terminals 2 and 4, so that $I_1=-I_3$ and $I_2=-I_4$. Then the pair of currents I_1 and I_2 are related to the voltage *differences* $V_{13}=e(\mu_1-\mu_3)$ between terminals 1 and 3 and $V_{24}=e(\mu_2-\mu_4)$ between terminals 2 and 4 through the conductance matrix α:

$$I_1=\alpha_{11}V_{13}-\alpha_{12}V_{24}, \quad I_2=-\alpha_{21}V_{13}+\alpha_{22}V_{24}. \quad (4.3)$$

Explicit expressions for the α coefficients in terms of scattering probabilities are given in Ref. 23. To determine the effective resistance of the array, one applies a current across terminals 1 and 3, and reads the voltage across 2 and 4, without drawing a current in terminals 2 and 4. Setting $I_2=0$ in Eq. (4.3) yields the effective resistance

$$V_{24}/I_1=\alpha_{12}/(\alpha_{11}\alpha_{22}-\alpha_{12}\alpha_{21}). \quad (4.4)$$

Figure 5 plots this resistance as a function of the Fermi energy E_F for the same array of eight T's considered above, for the same energy range $E_1<E_F<E_2$. Near either threshold the resistance diverges, since the probability for traversing the array vanishes, as in Fig. 3. At intermediate values of E_F, the scattering resonances are apparent as sudden increases in resistance. Near these resonances, the resistance can even take *negative* values. This result follows from the scattering properties detailed above. Away from resonance, current incident from terminal 1 has a good chance of flowing directly into the leads leading into terminal 2, thereby accumulating charge there and generating a potential difference between 2 and 4. On resonance, however, transport into these leads diminishes and charge carriers may have a better chance of reaching terminal 4, reversing the potential difference. Notice also that away from resonance, say near $E_F=250$ meV, the resistance remains nearly flat and has a value of $\sim h/2e^2$, the quantum unit of resistance. Thus the bend in the T acts like a constriction, quantizing the flow of electrons.[24]

The effective resistance plotted in Fig. 5 refers to the *Ohmic* resistance, for which the current is a linear function of the voltage difference. At higher potential differences, the difference in chemical potentials, $\mu_2-\mu_1$, covers a range of Fermi energies. If this range grows to include one of the resonances in Fig. 5, this resonance will impact the current-voltage characteristics of the device. The evaluation of current and voltage in this case follows as above, only now the contributions to the currents in Eq. (4.1) at each scattering energy must be integrated over the energy range $\mu_1<E<\mu_2$.[22] This integration assumes zero temperature, so that the chemical potentials μ_1 and μ_2 represent sharp limits of integration.

Figure 6 shows a resulting I-V curve for larger potential difference. The figure begins at $V_{24}=0$ with $\mu_1=\mu_2=E_F=360$ meV, and raises μ_2 through the resonance at ~ 400 meV in Fig. 5. The current I_1 rises linearly for low values of V_{24}, meaning that the resistance is Ohmic. At higher V_{24}, the I-V curve suddenly bends downward, signaling a region of negative differential resistance between 30 and 50 millivolts of applied voltage. The resistance then becomes positive again as μ_2 rises further, incorporating the large resonance feature of Fig. 5.

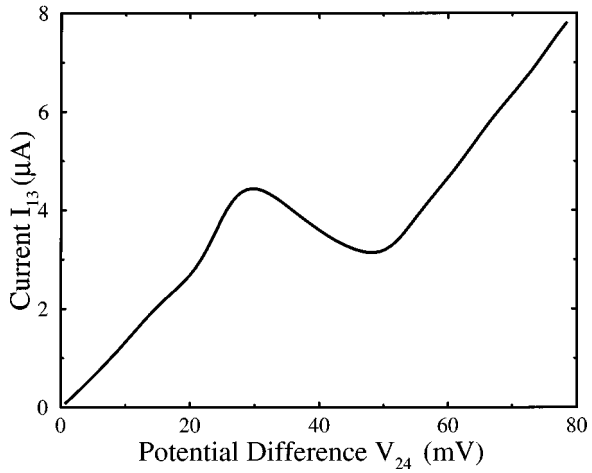

FIG. 6. Zero-temperature I-V diagram for an array of eight T's, exhibiting negative differential resistance between 30 mV and 50 mV of applied voltage.

Negative differential resistance has long been predicted[25] and was recently observed[26] in semiconductor superlattice structures. In superlattices the phenomenon arises from Bragg reflection of conduction electrons with the periodic structure. The present case of the T array contains the additional feature that electrons Bragg reflected from the array do not necessarily disappear back into the incident terminal, but have a chance of appearing in a different terminal altogether. The nonlinear I-V characteristics of a deflective T array might then be put usefully to work in device applications where a switch is required to shunt the current one way or another.

ACKNOWLEDGMENTS

I would like to thank G. Bryant, B. Esry, C. Greene, D. Jin, and P. Julienne for useful discussions. This work was supported by the NRC.

APPENDIX: THE EIGENCHANNEL R-MATRIX METHOD

The eigenchannel R-matrix method is a familiar and powerful computational tool in atomic collision theory, but is largely unknown among condensed matter physicists. We therefore sketch in this Appendix the basic elements of the method. More details can be found in Sec. III A of Ref. 15.

First it is important to note that a scattering problem, like the one presented by the T junctions here, seeks solutions to the Schrödinger equation at a certain fixed total energy E, with suitable boundary conditions for incoming and outgoing waves at infinite distances from the scattering region, as expressed by Eq. (2.5). As an intermediate step, however, we

are free to construct a set of wave functions satisfying *any* convenient boundary conditions (that is, computationally convenient). These solutions, to be denoted ψ_β below, can then be superposed as necessary to satisfy the physical scattering boundary conditions.

The R-matrix method constructs a useful intermediate set of wave functions as follows. First we envision a region of space A that contains the scattering region. A comprises a three-dimensional volume in the electron-atom scattering process described in Ref. 15 but will be a two-dimensional area in the 2D scattering problem of this paper. The shape of A is arbitrary, but it must be sufficiently large that the wave function *outside* of A can be expanded into known functions, e.g., those described in Eqs. (2.2) and (2.3) in the T example.

Inside the region A we could specify boundary conditions for the wave function and its derivative on the boundary of A, which would determine a set of energy eigenvalues E. Instead, for the scattering problem we specify the total energy E in advance, and so can choose only one boundary condition. Letting n represent the outward normal coordinate on A's surface, the R-matrix boundary condition demands that the outward normal logarithmic derivative,

$$b(E) = -\frac{\partial \ln(\psi)}{\partial n} = -\frac{1}{\psi}\frac{\partial \psi}{\partial n}, \tag{A1}$$

remain uniform over the boundary of A. Choosing the logarithmic derivative boundary condition greatly simplifies the subsequent matching to the scattering wave functions (2.5). We emphasize that these boundary conditions are temporary, and serve only to simplify the calculation. The complete scattering wave functions will not usually possess constant b along A's boundary.

To derive a variational expression for b, we first write the mean energy for an arbitrary real trial wave function ψ as

$$E = \frac{\int_A \psi(-\hbar^2/2m^*\vec{\nabla}^2\psi + U\psi)\,dA}{\int_A \psi^2\,dA}. \tag{A2}$$

Here a potential U has been inserted, anticipating future applications of the method to problems beyond the T. Applying Green's theorem in two dimensions reduces the Laplacian in Eq. (A2) to yield

$$E = \frac{\hbar^2/2m^*\left[\int_A \vec{\nabla}\psi\cdot\vec{\nabla}\psi\;dA - \int_l \psi(\partial\psi/\partial n)\,dl\right] + \int_A \psi U \psi\;dA}{\int_A \psi^2\,dA}. \tag{A3}$$

This reduction results in a line integral around the boundary l of the region A. Substituting the requirement (A1), we find an expression for the logarithmic derivative

$$b(E) = \frac{-\int_A \vec{\nabla}\psi\cdot\vec{\nabla}\psi\;dA + 2m^*/\hbar\int_A \psi(E-U)\psi\;dA}{\int_l \psi^2 dl}. \tag{A4}$$

For fixed E, Eq. (A4) is a variational expression for b, that is, Eq. (A4) is stationary with respect to small variations of the wave function ψ from a true solution to the Schrödinger equation with boundary conditions (A1). We exploit this circumstance by expanding the exact solution in a basis ϕ_k,

$$\psi = \sum_k \phi_k Z_k. \tag{A5}$$

In terms of this basis, the variational expression (A4) becomes (after ''reversing'' Green's theorem to recover the Laplacian)

$$b(E) = \frac{\sum_{kk'} Z_k \Gamma_{kk'} Z_{k'}}{\sum_{kk'} Z_k \Lambda_{kk'} Z_{k'}}, \tag{A6}$$

where

$$\Gamma_{kk'} = \frac{2m^*}{\hbar^2}\int_A \phi_k(E-H)\phi_{k'}\,dA - \int_l \phi_k \frac{\partial \phi_{k'}}{\partial n}\,dl \tag{A7}$$

and

$$\Lambda_{kk'} = \int_l \phi_k \phi_{k'}\,dl. \tag{A8}$$

Determining b and ψ variationally then amounts to setting all partial derivatives $\partial b/\partial Z_k$ equal to zero, which leads to a linear system that is conveniently expressed as a generalized eigenvalue problem,

$$\Gamma\vec{Z} = b\Lambda\vec{Z}, \tag{A9}$$

as described in Sec. II A.

Let us remark that, owing to the variational nature of Eq. (A6), *any* basis set is capable of making an estimate for the

eigenvalues b_β and eigenfunctions ψ_β of Eq. (A9). In practice, some of the ϕ_k must be nonvanishing on the boundary of A, to allow for finite values of the logarithmic derivative (A1), but the choice of basis is otherwise arbitrary. In particular, the ϕ_k do not have to form an orthogonal set. As is usually the case with variational methods, a sure way of achieving convergence in b_β and ψ_β is to increase the size of the basis.

*Electronic address: bohn@fermion.colorado.edu

[1] Y. Avishai and Y. B. Band, Phys. Rev. B **41**, 3253 (1990); F. Sols, M. Macucci, U. Ravaioli, and K. Hess, J. Appl. Phys. **66**, 3892 (1989); H. Wu, D. W. L. Sprung, J. Martorell, and S. Klarsfeld, Phys. Rev. B **44**, 6351 (1991).

[2] M. Macucci and K. Hess, Phys. Rev. B **46**, 15 357 (1992); Y. S. Joe, R. M. Cosby, M. W. C. Dharma-Wardana, and S. E. Ulloa, J. Appl. Phys. **76**, 4676 (1994); Z.-L. Ji and K.-F. Berggren, Phys. Rev. B **45**, 6652 (1992).

[3] Y. Wang, J. Wang, and H. Guo, Phys. Rev. B **49**, 1928 (1994); H. U. Baranger and P. A. Mello, Phys. Rev. Lett. **73**, 142 (1994).

[4] C.-K. Wang, K.-F. Berggren, and Z.-L. Ji, J. Appl. Phys. **77**, 2564 (1995); H. Xu, Phys. Rev. B **47**, 9537 (1993); A. A. Kiselev and U. Rössler, *ibid.* **50**, 14 283 (1994).

[5] J. Wang and H. Guo, Appl. Phys. Lett. **60**, 654 (1992); J. Wang, Y. J. Wang, and H. Guo, Phys. Rev. B **46**, 2420 (1992).

[6] C. Kittel, *Introduction to Solid State Physics*, 6th ed. (Wiley, New York 1976), Chap. 7.

[7] L. N. Pfeiffer *et al.*, Appl. Phys. Lett. **56**, 1697 (1990); H. L. Stormer, L. N. Pfeiffer, K. W. West, and K. W. Baldwin, in *Nanostructures and Mesoscopic Systems*, edited by W. P. Kirk and M. A. Reed (Academic, Boston, 1992).

[8] Y. C. Chang, L. L. Chang, and L. Esaki, Appl. Phys. Lett. **47**, 1324 (1985); A. R. Goñi *et al.*, *ibid.* **61**, 1956 (1992).

[9] W. Wegscheider *et al.*, Phys. Rev. Lett. **71**, 4071 (1993); Physica B (Netherlands) **227**, 390 (1997); G. W. Bryant, P. S. Julienne, and Y. B. Band, Superlattices Microstruct. **20**, 601 (1996).

[10] Ç. Kurdak, A. Zaslavsky, D. C. Tsui, M. B. Santos, and M. Shayegan, Appl. Phys. Lett. **66**, 323 (1995).

[11] N. F. Mott and H. S. W. Massey, *The Theory of Atomic Collisions*, 3rd ed. (Oxford, Clarendon, 1965).

[12] E. P. Wigner, Phys. Rev. **70**, 15 (1946).

[13] U. Fano and A. R. P. Rau, *Atomic Collisions and Spectra* (Academic, Orlando, 1986).

[14] P. G. Burke and K. A. Berrington, *Atomic and Molecular Processes – an R-matrix Approach* (Institute of Physics Publishing, Bristol, 1993).

[15] M. Aymar, C. H. Greene, and E. Luc-Koeing, Rev. Mod. Phys. **68**, 1015 (1996).

[16] C. S. Lent and D. J. Kirkner, J. Appl. Phys. **67**, 6353 (1990).

[17] C. H. Greene, Phys. Rev. A **28**, 2209 (1983).

[18] J. H. Wilkinson, *The Algebraic Eigenvalue Problem* (Oxford, Clarendon Press, 1965).

[19] H. Feshbach, Ann. Phys. (N.Y.) **19**, 287 (1962).

[20] S. Gasiorowicz, *Quantum Physics* (Wiley, New York, 1974).

[21] R. Landauer, IBM J. Res. Dev. **1**, 223 (1957); Philos. Mag. **21**, 863 (1970).

[22] H.-L. Engquist and P. W. Anderson, Phys. Rev. B **24**, 1151 (1981); M. Büttiker, Y. Imry, R. Landauer, and S. Pinhas, *ibid.* **31**, 6207 (1985).

[23] M. Büttiker, Phys. Rev. Lett. **57**, 1761 (1986).

[24] D. A. Wharam *et al.*, J. Phys. C **21**, L209 (1988); B. J. van Wees *et al.*, Phys. Rev. Lett. **60**, 848 (1988).

[25] L. Esaki and R. Tsu, IBM J. Res. Dev. **14**, 61 (1970).

[26] A. Sibille, J. F. Palmier, C. Minot, and F. Mollot, Appl. Phys. Lett. **54**, 165 (1989); H. T. Grahn, K. von Klitzing, K. Ploog, and G. H. Döhler, Phys. Rev. B **43**, 12 094 (1991); F. Beltram *et al.*, Phys. Rev. Lett. **64**, 3167 (1990).